A Numerical Investigation of the Effects of Inverted Drop Test Methods on PMHS Spine Response

Garrett A. Mattos, Raphael H. Grzebieta

Abstract Experimental testing with post mortem human subjects is costly and complex. Test methods that reduce the cost and increase the repeatability are favourable, although they may affect test outcomes. This study aims to improve the understanding of how test conditions affect PMHS responses related to axial compression spine injury. Select inverted head-first impact experiments from the literature were reconstructed in a simulated environment using a detailed Finite Element model of the human body, the THUMS. Test conditions such as specimen constraints, and test equipment setup and THUMS characteristics, such as mass and position were varied within each test protocol to assess inter- and intra-test effects. Test outcomes were evaluated and compared based on both the kinetic and kinematic response of THUMS. Constraint of T1 resulted in impact forces twice that recorded in otherwise equivalent inverted drop tests without constraints. The results of the simulations indicate that the introduction of unnatural boundary conditions is likely to interfere with the fidelity of injury production and response. These findings can assist in the development of future test methods to ensure that accurate results are obtained in the most repeatable and reproducible manner without unnecessary extraneous effects.

Keywords finite element, sensitivity, spine injury, THUMS.

I. INTRODUCTION

Experimental testing with post mortem human subjects (PMHSs) forms the biomechanical foundation from which injury criteria, and subsequently, injury mitigation techniques can be developed [1]. The cost and complexity involved in conducting experiments with PMHSs, as well as the low availability of acceptable specimens, makes it paramount that each test produces as much valid data as possible. The ability to generate meaningful and useful biomechanical response data from an experiment is based on the employed test method. Experiments investigating spinal compression injury have been conducted using a variety of test setups including full-body inverted drop tests of seated and standing PMHSs [2-4], linear and pendulum impacts to supine PMHSs [5-7], inverted drop tests of constrained head-neck complexes [8-9] all with differing levels of constraint, pre-compression of the spine, impactor padding, and head-neck orientations defined.

While the use of full-body PMHSs can provide a biofidelic response to impact, it precludes the ability to directly measure, without altering, the internal response and loads. New technologies such as high speed X-ray are helping to visualise the internal responses of the PMHSs [10], though setup is challenging and useful results are not guaranteed. On the other hand, experiments using reduced components, such as a head-neck complex [8], allow for the direct measurement and observation of the response of the spine. Component tests are also generally performed on a smaller scale, with greater control of constraints and boundary conditions that provides for a highly repeatable test. The addition of these boundary conditions, however, is likely to alter the response of the specimen.

The objective of this study was to investigate the effect that select test conditions have on the spinal compression-injury response resulting from inverted head-impacts using the Total HUman Model for Safety (THUMS). The THUMS has undergone extensive validation with regard to head and spine response against multiple PMHS tests which are summarised in [11]. Additionally, the use of finite element (FE) simulation in this sensitivity study provides an efficient method of assessing the effects of discrete changes in test parameters. The use of THUMS supports this objective in that it allows for a comparison of identical specimen attributes across all simulated test conditions.

G. A. Mattos is a Post-Doctoral Research Associate (+61 9385 4741, g.mattos@unsw.edu.au) and R. H. Grzebieta is Professor of Road Safety at the Transport and Road Safety (TARS) Research Centre at the University of New South Wales in Sydney, Australia.

II. METHODS

The AM50 Total HUman Model for Safety (THUMS) v4.01 [12], was used to simulate inverted head impacts following two test methods; a component test as outlined by [8], and a full-body inverted drop as performed by [4], Figure 1. The LS-DYNA nonlinear explicit finite element solver version R7.0.0 (Livermore Software Technology Corporation) was used for all simulations. The THUMS has previously been validated against component-style inverted head impact tests [8] and found to provide reasonable kinetic and kinematic response [11]. Although the THUMS supports element failure, which causes finite elements to be deleted after they have reached a threshold strain value, and has predefined strain threshold values for the skull bones, this option was turned off so that potential simulated fractures would not affect the calculated peak load values.

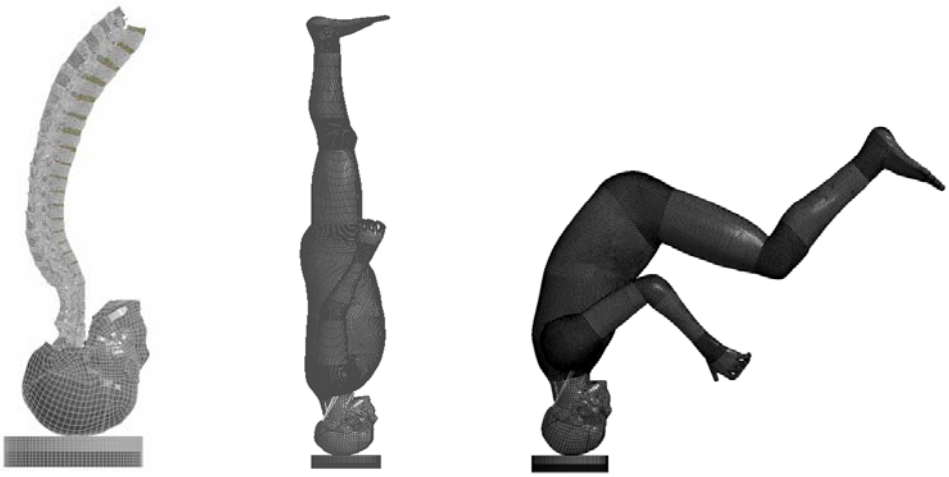

Fig. 1. Test setup configurations for component (left), full-body standing (middle), and full-body seated (right) inverted drop tests.

In both test methods, the vertex of the THUMS head impacted the centre of a rigid plate. For impacts in which padding was defined, a 25.4-mm-thick energy-absorbing styrenic thermoplastic foam (IMPAXX700) [13] with a coefficient of friction = 0.4, commonly used in headliner applications, was simulated [14]. The standard position of the *seated* THUMS is such that the Frankfurt plane is parallel to the ground and the angle of the superior endplate of T1 is 21.5 deg. The angle of T1 in the *standing* THUMS is 14.3 deg. The ligamentous head-neck complex used by [8] was modelled by modifying the *seated* THUMS by removing all parts except the head and bony- and ligamentous-features of the spine.

In the component tests, a boundary condition was applied which restricted motion of the constrained vertebra to the vertical direction, to match the constraints applied by the test apparatus used by [8]. To simulate the carriage mass for the component tests, the constrained vertebra was made rigid and its density was defined such that its mass was equivalent to that specified in the protocol. All vertebrae located inferior to the constrained vertebrae were deleted. For each component test the carriage mass, impact velocity, constraint location, and padding option were defined as summarised in Table I. Likewise, the padding option, THUMS position, and impact velocity prescriptions are also listed in Table I.

Vertebral loads were calculated using section forces defined by cross-sections that ran transversely through the middle of select vertebrae: C1, C5, C7, T1, T4, T8, T12, and L4. Head force was calculated using the contact force between the THUMS head and the rigid plate. All load data was output at 10,000 Hz and filtered with the SAE CFC 1000. The principal strain for each shell element representing a segment of cortical bone in the cervical spine was also output at 10,000 Hz. The peak stain reached by each element was averaged (an average of 3822 values) to establish a measure, *average maximum strain*, of fracture risk for each test. The displacement of each vertebra was calculated from the resulting d3plots which were output at every 0.001 s.

Statistical Analysis

One-way analysis of variance (ANOVA) tests were conducted to evaluate the effect of each test parameter on the kinetic and kinematic response of the THUMS. Multiple linear regressions were performed to predict THUMS response measures based on select test parameters.

TABLE I
SUMMARY OF TEST CONDITIONS

Test method	Padding	Constraint	Position	Carriage mass (kg)	Impact velocities (m/s)
Component	-	T1		8	2, 3, 4, 5
Component	-	T1		16	2, 2.5, 3, 3.5, 4, 4.5, 5
Component	-	T1		32	2, 3, 4, 5
Component	-	L1		16	2, 3, 4, 5
Component	-	L5		16	2, 3, 4, 5
Component	Yes	T1		16	2, 3, 4, 5
Component	Yes	T1		32	2, 3, 4, 5
Component	Yes	L1		16	2, 3, 4, 5
Component	Yes	L5		16	2, 3, 4, 5
Full-body	-	n/a	Standing	n/a	2, 3, 4, 5
Full-body	-	n/a	Seated	n/a	2, 3, 4, 5
Full-body	Yes	n/a	Standing	n/a	2, 3, 4, 5
Full-body	Yes	n/a	Seated	n/a	2, 3, 4, 5

III. RESULTS

General Descriptive Results

A total of 55 inverted head-impacts were simulated, including 39 component-tests and 16 full-body tests. While the results of all 55 simulations are used and included in all statistical analyses, for ease of comparison a *base set* of 5 simulations will be referred to in this section of general descriptive results. The conditions of this *base set* are outlined in the first 5 columns of Table II.

The peak force calculated at T1 for *all* simulations ranged from 787.69 N to 6074.32 N. A summary of the maximum forces calculated at select vertebrae for the *base set* is given in Table II. Peak forces measured at T1 in the component test with T1 constraint were 1.8 and 2.2 times greater those measured in the full-body seated and standing tests, respectively.

TABLE II
SUMMARY OF MAXIMUM FORCES BY CONSTRAINT AND MEASUREMENT LOCATION

	Conditions				Maximum force (N)						
Type	Constraint	Mass (kg)	Velocity (m/s)	Padding	C1	C5	T1	T4	T8	T12	L4
Component	T1	16	3	Yes	2287	4189	4539				
Component	L1	16	3	Yes	1318	1225	1271	1480	1608	1448	
Component	L5	16	3	Yes	985	882	986	1106	1202	937	888
Full-body	Seat	n/a	3	Yes	1765	1928	2088	1988	1442	779	518
Full-body	Stand	n/a	3	Yes	2053	2572	2539	2602	2457	1618	1313

The time-histories of the T1 and head impact forces for the *base set* are presented in Figure 2. The behaviour of the T1 force curve was different for each simulation with regard to peak value and time-to-peak value. The contact force between the THUMS head and rigid plate was bimodal. The maximum force calculated in the first peak was nearly identical for *all* simulations with equal initial velocity and padding parameters. The value and time of the second peak varied depending on the constraint option. In the component tests, moving the constraint caudally had the effect of reducing and delaying 2nd-peak head forces. The inverted impacts of full-body seated and standing THUMS resulted in similar curves with a slight reduction and delay of peak head force for the seated model. In the component tests the head rebounded fully or partially off the plate, while in the full body tests the head continued to load the plate after the initial impact.

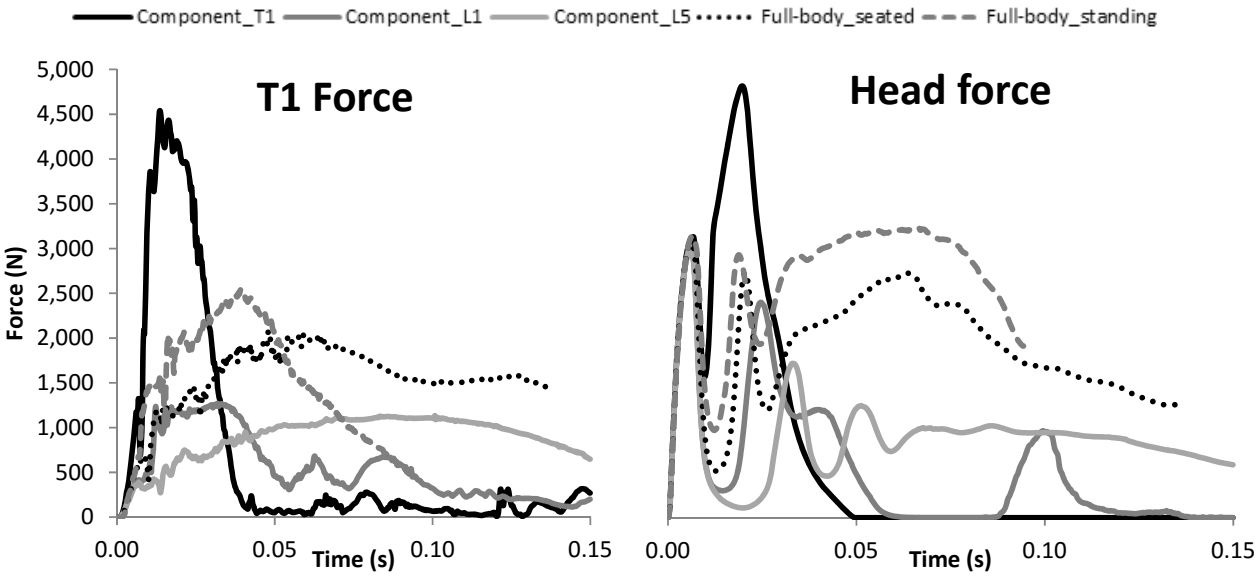

Fig. 2. Force vs time curves for T1 (left) and head contact (right) for *base set* of simulations

The motion of the spine was recorded from the d3plots and visualisations for the *base set* of simulations are presented in Figure 3. To allow for the largest possible reproduction of images in Figure 3, only the unconstrained vertebrae are shown. In the component test with T1 constraint, far left column in Figure 3, the kinematics of the cervical spine mimicked that of a spring with a loading phase during which the spine went into flexion followed by an unloading phase in which the spine returned to its pre-deformed shape.

The constraint at L1 resulted in extreme hyper-flexion of the cervical spine. Throughout the loading phase ($0 < t < 0.05$), the maximum relative transverse displacement between C1 and T1 was 11 mm, both displacing anteriorly as the cervical spine flexed. As the T1 and head force dissipated ($t = 0.04$ s) the head rotated posteriorly, further increasing the extent of flexion.

The kinematic response of the cervical spine in the component test with a L5 constraint closely matched that observed in the full-body seated and standing simulations. Initial loading caused the spine to flex ($0 < t < 0.02$) resulting in increased lordosis and kyphosis of the cervical and thoracic spines, respectively. As the loading increased ($0.02 < t < 0.07$) T1 displaced posteriorly preventing the extreme hyperflexion as seen in the L1 constraint from occurring. Slightly more flexion in the cervical spine was observed for the standing model than the seated model. Additionally, in the standing model, the natural lordosis of the lumbar spine was maintained. No such lordosis of the lumbar spine was present in the seated model.

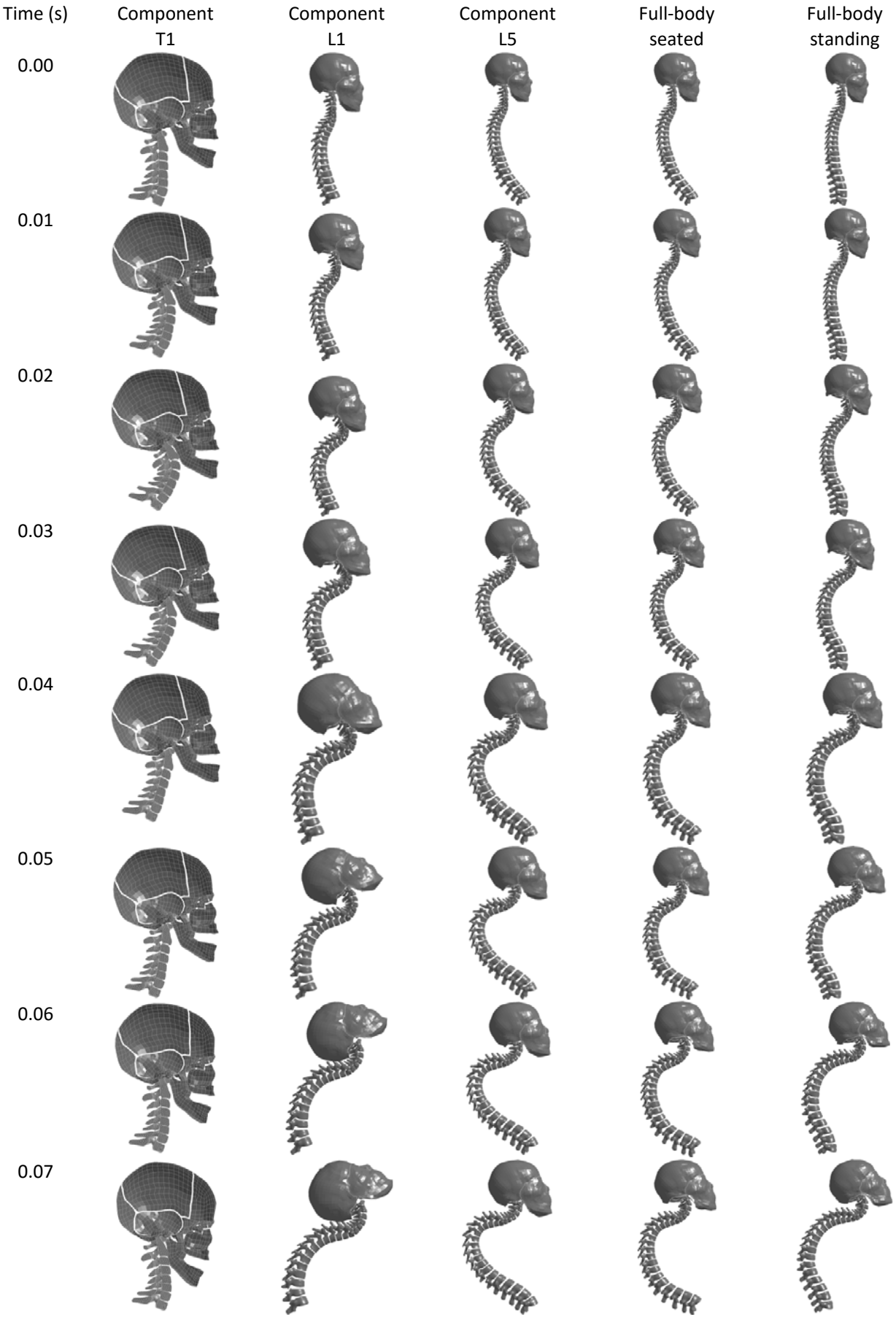

Fig. 3. Visualizations of spine (C1-T1) kinematics response for 3 m/s padded impact tests 16 kg carriage mass.

Statistical Analysis

One-way ANOVA tests were conducted to evaluate the effect of each test parameter on the kinetic and kinematic response of the THUMS. The ANOVA demonstrated that, for the component test method, the effect of carriage mass on peak T1 force was significant, F (2, 20) = 4.15, p = 0.031. The effect of mass was significant for peak forces calculated at every vertebra as well as for the time at which the peak force occurred. As the carriage mass was increased, the peak force and time to peak force also increased as demonstrated in Figure 4.

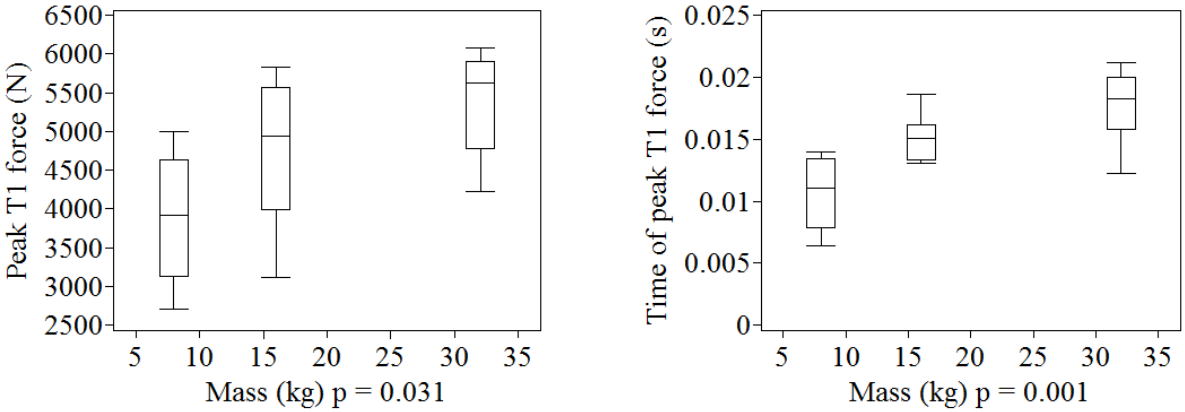

Fig. 4. Box plots of peak force at T1 (left) and time of peak force at T1 (right) by carriage mass for all component tests with T1 constraint.

Peak vertebral force and time of peak vertebral force were also significantly correlated with the vertebral constraint location for the component tests, Table AI and Table AII. The peak force calculated at each vertebra decreased as the constraint moved caudally. At the same time, the time-to-peak force increased respectively. For the full-body simulations, the THUMS position, e.g. seated or standing, had a significant effect on the peak forces in the vertebrae, Table AI. The standing position was significantly associated with greater forces calculated at C5, C7, T8, T12, and L4. The standing position was also significantly associated with a lower time-to-peak for most vertebrae below T1; there was no significant difference in the timing of peak forces measured in the cervical spine.

The average maximum strain followed the same general trend as the peak force values. The ANOVA demonstrated that the effects of constraint type on both the average maximum strain and the average time of maximum strain for the cervical spine were significant, F(4, 50) = 8.22, p = <.0001; F(4, 50) = 34.85, p = <.0001, Figure 5. Greater values of strain were calculated for simulated tests with T1 constraint than for all other conditions. The average time the maximum strain occurred for each element increased with increasing inferior constraint for the component tests.

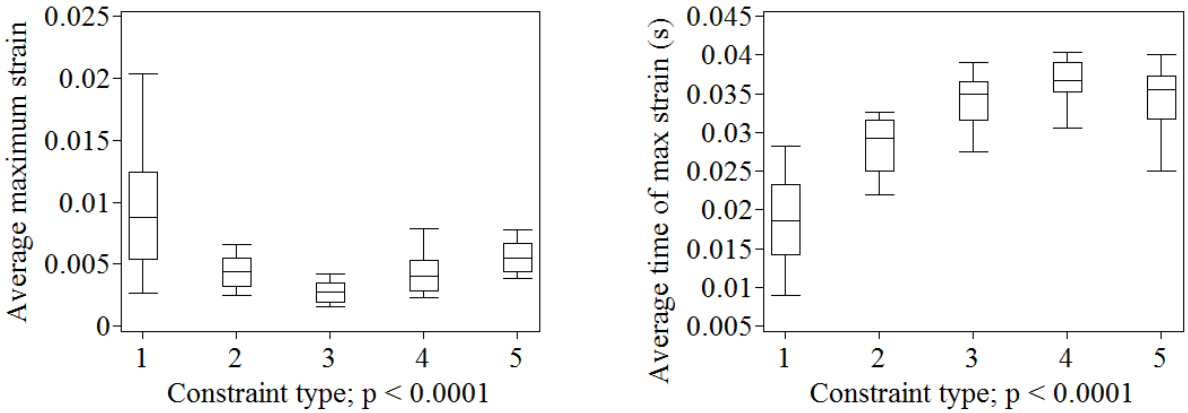

Fig. 5. Box plots of average maximum element strain in the c-spine (left) and average time of maximum strain in the c-spine (right) by carriage mass for all simulations

Greater impact velocity was significantly associated with increased peak vertebral forces for impacts of a

given type or constraint, e.g. component test with T1 constraint. Impact velocity was not a significant predictor of peak vertebral force when all impacts types or constraint types were grouped together. While the effect of impact velocity on time to peak force was not generally significant for the component tests, it was found to be significant for the lower cervical spine in the full body tests.

One-way ANOVA tests were conducted to evaluate the effect of the test constraint parameter on the anterior displacement of the cervical spine vertebrae. The analysis showed that the effect of constraint location on cervical vertebrae displacement was significant for the component tests, $F(2, 36) = 159.45$, $p = <.0001$; ANOVA results are reported for displacement of C7. Likewise the effect of THUMS position, e.g. seated or standing, significantly affected the displacement of the cervical vertebrae, $F(1, 14) = 25.54$, $p = 0.0002$; ANOVA results reported for displacement of C7. In the component tests the greatest displacement, 143.3 mm on average for C7, was observed for those conducted with L1 constraint, Figure 6. The tests constrained at T1 and L5 recorded 12.1 mm and 25.4 mm on C7 anterior displacement on average, respectively. In the full-body simulations, the standing THUMS presented with the greatest amount of cervical spine displacement; 59.6 mm vs 24.1 mm on average for C7, Figure 6.

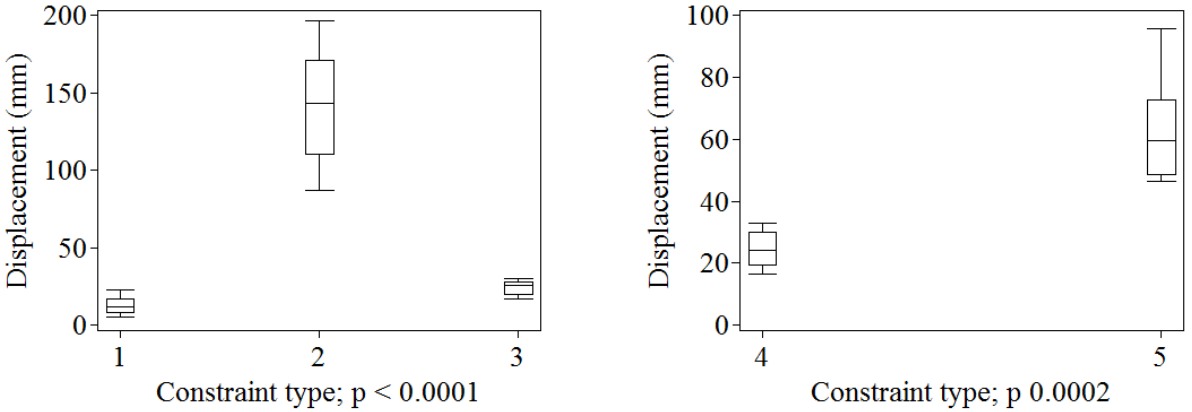

Fig. 6. Box plots of maximum anterior displacement of C7 plotted against constraint type for component tests (left) and full-body tests (right); constraint coded as 1 = T1, 2 = L1, 3 = L5, 4 = seated, and 5 = standing.

Three multiple-linear-regression analyses were carried out to predict THUMS response measures based on select test conditions. Three models were produced based on different groupings of the simulated test types. The first model included only *component-test* simulations and predicted the peak force at T1 based on carriage mass, padding option, impact velocity, and constraint location. A significant regression equation was found ($F(4,34) = 63.77$, $p < .0001$), with an R2 of .883: The predicted peak force at T1 is:

$$\text{T1 force (N)} = 3648.78 + 63.58\,(\text{mass}) - 166.14\,(\text{pad}) + 481.49\,(\text{velocity}) - 1904.31\,(\text{constraint}), \quad (1)$$

where mass is measured in kg, pad is coded as 1 = padded, 0 = not padded, velocity is measured in m/s, and constraint location is coded as 1 = T1, 2 = L1, and 3 = L5. With all other factors being equal, the peak force at T1 increased by 63.58 N and 481.49 N for each unit increase in carriage mass and impact velocity, respectively. A more inferior constraint of the spine both resulted in independent decreases in peak T1 force. All variables, except padding, were significant predictors of peak T1 force in the model.

A second multiple linear regression was calculated to predict peak T1 forces for the *full-body* simulations. The model was found to be significant ($F(3,12) = 63.06$, $p <.0001$), with an R2 = .940:

$$\text{T1 force (N)} = 592.00 + 201.65\,(\text{pad}) + 379.52\,(\text{velocity}) + 500.48\,(\text{constraint}), \quad (2)$$

where pad and velocity are defined as above and constraint is coded as 1 = standing, 0 = seated. With all other factors being equal, the model predicts an increase of 201.65 N in peak T1 force for a padded vs non-padded impact. A one-unit increase in velocity increased the peak force at T1 by 379.51 N and the standing full-body model produces peak T1 forces 500.48 N greater than the seated model. All variables were significant

predictors of peak T1 force.

A third multiple linear regression was computed to predict peak T1 forces for *all* simulations and was also found to be significant ($F(5, 49) = 32.21$, $p < .0001$), $R2 = .767$:

T1 force (N) =

$$3008.12 - 711.28\,(\text{type}) + 73.01\,(\text{mass}) - 129.29\,(\text{pad}) + 451.05\,(\text{velocity}) - 1558.89\,(\text{constraint}), \quad (3)$$

where all variables are coded as above except for type; 1 = full-body, 0 = component, and constraint; 1 = T1, 2 = L1, 3 = L5, 4 = seated, and 5 = standing. Carriage mass, impact velocity, and constraint location were all significant predictors of peak T1 force while padding option and test type were not significant.

IV. DISCUSSION

Each test parameter was found to significantly affect one or more kinetic or kinematic responses of the THUMS in the simulated inverted head impact tests. The motion of the cervical spine was demonstrated to be affected by test type and constraint location. The T1 constraint in the component tests essentially increased the rigidity of the cervical spine which resulted in greater forces to develop during the impact [15]. As constraints were moved caudally, or removed altogether, peak forces tended to decrease as the spine was able to flex and disperse the load away from its axis as demonstrated in experimental tests reported in [16].

While the component tests where L5 was constrained demonstrated the greatest similarity to the full-body tests with regard to cervical spine kinematics, there would be no practical advantage to conducting such a test. Unlike a constraint at T1, a boundary condition applied at L5 would offer little increase in repeatability over a full-body test. Additionally, it would require custom mounts that would add to the complexity of the experiment. The ability to measure the biodynamic response of the specimen would be no different than for a full-body test.

Some differences were noted in the response of full-body standing and seated THUMS. The choice of PMHS position in inverted head impacts is non-trivial and should be based on the conditions the test aims to replicate. The seated position is an obvious choice with regard to conducting tests related to spine injury in vehicle rollover; however tests aiming to replicate the injury mechanisms in pool diving injuries may benefit from using a PMHS in a standing position. In the above simulations the standing THUMS experienced a more severe impact for equal test parameters as compared to the seated THUMS. This is likely due to the more upright posture of the standing THUMS, T1 angle = 14.3 deg vs 21.5 deg, which results in loading more aligned with the axis of the cervical spine [17]. Additionally the centre-of-gravity (CoG) of the standing THUMS is 11.6 mm anterior of the centre of C1, while the CoG of the seated THUMS is 105.3 mm anterior of the centre of C1. The spine of the seated THUMS, therefore, has to cope with a lower effective inertia.

The time history of the head force in the above simulations was similar to physical tests performed elsewhere [4][10]. The results here support the idea that the initial peak in the bimodal head force curve is a function of the mass and velocity of the head-neck complex, and is likely not directly indicative of spine fracture risk [8]. On the other hand, velocity was not a significant predictor of peak vertebral force, though test type and constraint were. This implies that the boundary conditions have a stronger effect on the biodynamic response of the spine than the kinematic conditions and should be chosen carefully to ensure that the intended impact scenario is replicated accurately. Future work in this area will extend the test conditions to identify a protocol that provides the optimal balance between test fidelity and repeatability; however, these results suggest that it is unlikely component level testing will meet the fidelity requirements.

The limitations of this work should be noted. The strength of this work lies in evaluating relative risks based on measured response and cannot be used to identify or predict absolute measures of injury risk. The lack of active musculature in the THUMS precludes it from replicating the responses of living humans. While this study may demonstrate the difference in response for PMHSs, it may not reflect differences in response for living humans that experience similar loading conditions with or without implied constraints. The THUMS only represents one subject, and the results may or may not be able to be generalised to the full population. Furthermore, the biodynamic response of the THUMS spine, though comparable to experimental data, could be

improved; however, any improvement is not expected to alter the overall conclusions of this work.

V. CONCLUSIONS

Fifty-five inverted head impact tests were simulated to quantify the effect of select test parameters on the biodynamic response of the cervical spine. All test parameters were found to significantly affect one or more kinetic or kinematic responses of the THUMS. The test parameters that had the greatest effect on the response of the cervical spine had to do with the constraint and position of the THUMS. An increase in constraint resulted in kinematic and kinetic responses that increasingly differed from the full-body responses.

VI. REFERENCES

[1] Crandall, J.R., Bose, D., et al. Human surrogates for injury biomechanics research. *Clinical Anatomy*, 2011. 24(3): p. 362-371

[2] Sances Jr, A., Yoganandan, N., et al., "Mechanisms of Head and Spine Trauma", pages 717-736, Aloray Publishers: Groshen, NY, 1986

[3] Yoganandan, N., Anthony Sances, J., et al., "Spine", pages 855-860, 1986

[4] Roberts, C. and Kerrigan, J. Injuries and kinematics: response of the cervical spine in inverted impacts. *Proceedings of 24th International Technical Conference on the Enhanced Safety of Vehicles*, 2015. Gothenburg, Sweden

[5] Alem, N.M., Nusholtz, G.S., and Melvin, J.W. Head and Neck Response to Axial Impact. *Proceedings of 28th Stapp Car Crash Conference*, 1984. Warrendale, PA

[6] Nusholtz, G.S., Melvin, J.W., Huelke, D.F., Alem, N.M., and Blank, J.G. Response of the Cervical Spine to Superior-Inferior Head Impacts. *Proceedings of 25th Stapp Car Crash Conference*, 1981. Warrendale, PA

[7] Culver, R.H., Bender, M., and Melvin, J.W. Mechanisms, Tolerances and Responses Obtained Under Dynamic Superior-Inferior Head Impact. Final Report. 1978.

[8] Nightingale, R.W., McElhaney, J.H., Richardson, W.J., and Myers, B.S. Dynamic responses of the head and cervical spine to axial impact loading. *Journal of Biomechanics*, 1996. 29(3): p. 307-318

[9] Pintar, F.A., Yoganandan, N., et al. Dynamic characteristics of the human cervical spine, in *39th Stapp Car Crash Conference*. 1995, Society of Automotive Engineers: Warrendale, PA, USA.

[10] Kerrigan, J., Foster, J.B., et al. Axial compression injury tolerance of the cervical spine: initial results. *Traffic Inj Prev*, 2014. 15(sup1): p. S265-S269

[11] Mattos, G.A., McIntosh, A.S., Grzebieta, R.H., Yoganandan, N., and Pintar, F.A. Sensitivity of head and cervical-spine injury measures to impact factors relevant to rollover crashes. *Traffic Inj Prev*, 2015. 16(sup1): p. S140-S147

[12] Shigeta, K., Kitagawa, Y., and Yasuki, T. Development of next generation human FE model capable of organ injury prediction, in *21st International Technical Conference on the Enhanced Safety of Vehicles*, NHTSA, Editor. 2009, NHTSA: Stuttgart, Germany.

[13] Dow Automotive, T. Finite element analysis with IMPAXX energy absorbing foams in headliner applications - Modeling instructions and material models for use in FMVSS201U head impact simulations. 2009.

[14] Slik, G., Vogel, G., and Chawda, V. Material model validation of a high efficiency energy absorbing foam, in *5th German LS-DYNA Forum*. 2006, DYNAmore GmbH: Ulm, Germany.

[15] Nightingale, R.W., Myers, B.S., McElhaney, J.H., Doherty, B., and Richardson, W.J. The influence of end condition on human cervical spine injury mechanisms. *Proceedings of SAE*, 1991.

[16] Pintar, F.A., Voo, L.M., Yoganandan, N., Cho, T.H., and Maiman, D.J. Mechanisms of hyperflexion cervical spine injury. *Proceedings of the International Research Council on the Biomechanics of Injury conference*, 1998. 26: p. 249-260

[17] Liu, Y.K. and Dai, Q.G. The Second Stiffest Axis of a Beam-Column: Implications for Cervical Spine Trauma. *Journal of Biomechanical Engineering*, 1989. 111(2): p. 122-127

VII. APPENDIX

The *p-values* resulting from one-way ANOVA tests assessing the significance of the effect of an independent variable, e.g. Mass, on a dependent variable, e.g. peak force at T1, are listed in Table A1 and Table A2. Some tests were performed on subsets of data, e.g. component tests, as described in the second column. Each cell represents an individual one-way ANOVA test, and is highlighted based on the level of significance.

TABLE AI
ONE-WAY ANOVA SIGNIFICANCE RESULTS: PEAK VERTEBRAL FORCE

Independent variable	Subset	Dependent variable = peak vertebral force							
		C1	C5	C7	T1	T4	T8	T12	L4
					(*p-value*)				
Mass	component tests	0.001	0.002	0.001	0.001		n/a		
Mass	T1 constraint	0.020	0.049	0.033	0.031		n/a		
Velocity	component tests	0.301	0.764	0.650	0.583	0.006	0.006	0.1162	0.080
Velocity	T1 constraint	0.021	0.019	0.003	0.003		n/a		
Velocity	full-body tests	<.0001	0.068	0.011	0.002	0.000	0.004	0.097	0.464
Constraint	component tests	<.0001	<.0001	<.0001	<.0001	0.029	0.037	0.005	n/a
Position	full-body tests	0.951	0.003	0.022	0.058	0.177	0.023	0.001	0.000
Type	all tests	0.120	0.110	0.082	0.032	0.000	0.020	0.807	0.838

p≥0.05	0.01≤p<0.05	p<0.01

TABLE AII
ONE-WAY ANOVA SIGNIFICANCE RESULTS: TIME OF PEAK VERTEBRAL FORCE

Independent variable	Subset	Dependent variable = time of peak vertebral force							
		C1	C5	C7	T1	T4	T8	T12	L4
					(*p-value*)				
Mass	component tests	0.138	0.174	0.134	0.092		n/a		
Mass	T1 constraint	0.005	0.314	0.003	0.001		n/a		
Velocity	component tests	0.572	0.813	0.992	0.887	0.876	0.921	0.971	n/a
Velocity	T1 constraint	0.499	0.012	0.645	.0679		n/a		
Velocity	full-body tests	0.081	0.005	0.011	0.000	0.730	0.704	0.586	0.269
Constraint	component tests	0.004	<.0001	<.0001	<.0001	<.0001	<.0001	<.0001	n/a
Position	full-body tests	0.555	0.950	0.123	0.3593	<.0001	<.0001	0.001	0.745
Type	all tests	0.002	<.0001	0.001	0.001	0.095	0.061	0.006	0.446

p≥0.05	0.01≤p<0.05	p<0.01